Centrum voor Wiskunde en Informatica

REPORT*RAPPORT*

MAS

Modelling, Analysis and Simulation

Modelling, Analysis and Simulation

A numerical study of an adaptive finite element method of lines approach for coupled reaction-diffusion equations in $\Omega - \partial\Omega$.

L. Ferracina

REPORT MAS-E0701 JANUARY 2007

Centrum voor Wiskunde en Informatica (CWI) is the national research institute for Mathematics and Computer Science. It is sponsored by the Netherlands Organisation for Scientific Research (NWO).
CWI is a founding member of ERCIM, the European Research Consortium for Informatics and Mathematics.

CWI's research has a theme-oriented structure and is grouped into four clusters. Listed below are the names of the clusters and in parentheses their acronyms.

Probability, Networks and Algorithms (PNA)

Software Engineering (SEN)

Modelling, Analysis and Simulation (MAS)

Information Systems (INS)

P.O. Box 94079, 1090 GB Amsterdam (NL)
Kruislaan 413, 1098 SJ Amsterdam (NL)
Telephone +31 20 592 9333
Telefax +31 20 592 4199

ISSN 1386-3703

A numerical study of an adaptive finite element method of lines approach for coupled reaction-diffusion equations in $\Omega - \partial\Omega$.

ABSTRACT
A numerical study of an adaptive finite element method of lines (AFEMOL) approach is presented for the approximation of the solution of a system of reaction-diffusion equations coupling species defined on a 2-dimensional domain Ω and species confined to the boundary of the domain $\partial\Omega$. In order to bound the energy norm of the space discretization error, in the AFEMOL the spatial mesh changes automatically at selected times when the underlying triangulation is refined in areas where it is needed. The decision of *when* and *where* to modify the mesh is based on the estimation of the space discretization error. The adaptive process and the a-posteriori explicit error estimation exploited in this note are a modification of the pioneer work developed by Bieterman and Babuschka in [Numer. Math. 40 (1982), 339], [Numer. Math. 40 (1982), 373], [J. Comput. Phys. 63 (1986), 33]. The primary interest, in the manuscript, is the effect of the coupling Ω–$\partial\Omega$ on the performance of the error estimator and the successive adaptive process. Our numerical results indicate that the global error estimators are accurate, the local error indicators are reliable and that the adaptive strategy successfully controls the space discretization error.

2000 Mathematics Subject Classification: 65M60, 65M20, 65M15
Keywords and Phrases: Adaptive finite element method of lines, reaction-diffusion equations, a-posteriori error estimation, coupling surface-domain, singular source terms.
Note: Work carried out under project MAS1.1 - ' PDEs in the life sciences '.

A numerical study of an adaptive finite element method of lines approach for coupled reaction-diffusion equations in $\Omega - \partial\Omega$

Luca Ferracina
CWI
P.O. Box 94079, 1090 GB Amsterdam, The Netherlands

ABSTRACT

A numerical study of an adaptive finite element method of lines (AFEMOL) approach is presented for the approximation of the solution of a system of reaction-diffusion equations coupling species defined on a 2-dimensional domain Ω and species confined to the boundary of the domain $\partial\Omega$.

In order to bound the energy norm of the space discretization error, in the AFEMOL the spatial mesh changes automatically at selected times when the underlying triangulation is refined in areas where it is needed. The decision of *when* and *where* to modify the mesh is based on the estimation of the space discretization error.

The adaptive process and the a-posteriori explicit error estimation exploited in this note are a modification of the pioneer work developed by Bieterman and Babuška in [Numer. Math. 40 (1982), 339], [Numer. Math. 40 (1982), 373], [J. Comput. Phys. 63 (1986), 33]. The primary interest, in the manuscript, is the effect of the coupling Ω–$\partial\Omega$ on the performance of the error estimator and the successive adaptive process. Our numerical results indicate that the global error estimators are accurate, the local error indicators are reliable and that the adaptive strategy successfully controls the space discretization error.

2000 Mathematics Subject Classification: 65M60, 65M20, 65M15.
Keywords and Phrases: adaptive finite element method of lines, reaction-diffusion equations, a-posteriori error estimation, coupling surface-domain, singular source terms.
Note: Work carried out under project MAS1.1 - ' PDEs in the life sciences '.

1. Introduction

1.1 The purpose of the paper

Reaction-diffusion processes occur in many branches of engineering, physics, biology and chemistry. Because in many cases these processes can be accessed experimentally only to a limited extent, often simulation models and their numerical solution are the only available option to study such phenomena. Many times these processes are modeled by initial boundary value problems (IBVP) in which the governing partial differential equations (PDEs), of the form

$$\frac{\partial A}{\partial t} - \nabla \cdot (D_A \nabla A) = R_A \quad \text{for } (x,t) \in \Omega \times (0,\infty), \tag{1.1.a}$$

are coupled only through the rate R_A at which chemical components react.

Solutions of reaction-diffusion problems of the form (1.1.a) may decay to steady states, oscillate in time or evolve as localized traveling wavefronts. An accurate numerical solution (at a reasonable cost) that capture such different behaviors is only possible through an adaptive procedure that automatically refines and coarses the space mesh and the time step only *when* and *where* it is needed – see, e.g., [21].

Much attention has been paid in the literature to adaptive finite element methods and a-posteriori error estimates for models of the form (1.1.a). An integrated space-time finite element method is presented, e.g., in [22],[23],[24],[27] where conforming finite elements are used for the space discretization and the time integration is carried out with the discontinuous Galerkin method. A different approach, called the (adaptive) finite element method of lines (FEMOL) was developed and analyzed by Bieterman and Babuška in [10],[11],[12] – see also [1],[2],[28],[29]. We refer also to [8], [31] and the excellent monograph by Ainsworth and Oden [3] for a clear introduction to error estimation and adaptive finite element methods.

In the FEMOL an IBVP for a system of PDEs is reduced through space discretization (i.e. the Galerkin method) into an initial value problem (IVP) for a system of ordinary differential equations

(ODEs). The IVP for the system of ODEs, which determine the nodal values of the solution, can then be efficiently solved by one of the available ODE methods (e.g. multistep methods or Runge-Kutta methods). In order to achieve a given level of accuracy, the adaptive FEMOL refines the space mesh in areas where it is needed. If these areas are located in different parts of the domain at different moments in time, it is desirable to modify the space mesh at various times. The decision of *when* and *where* to modify the mesh is based on an estimation of the space discretization error.

In this paper we consider the adaptive FEMOL for a more general model than (1.1.a) where additional coupled reaction-diffusion processes are confined to the boundary of the domain. This situation appears, for instance, when modeling catalysts, semiconductor components and membrane-bound biochemical pathways. In the last case – see, e.g., [25],[13] – we describe the time variation of each of the reacting species inside the cytosol via equations of the form (1.1.a) – where A is the volume concentration of any one of the species, the reaction rate R_A is obtained from the stoichiometry matrix and the corresponding rate coefficients of the biological network and the coefficients D_A are the corresponding diffusion rates. The species which are bound to the membrane of the cell can then be modeled by surface concentrations defined only on the boundary of the domain $\partial\Omega$. They also undergo diffusion as well as reaction:

$$\frac{\partial B}{\partial t} - \nabla \cdot (D_B \nabla B) = R_{AB} \quad \text{for } (x,t) \in \partial\Omega \times (0,\infty). \tag{1.1.b}$$

For the mass balance of the interior species, reactions at the boundary represent sink/source terms. The corresponding boundary conditions are obtained by equating the source/sink terms with the local fluxes on the boundary.

The primary interest, in the paper, is the effect of the coupling Ω–$\partial\Omega$ on the performance of the space error estimation when solving (1.1) with the adaptive FEMOL. In the manuscript we restrict our attention to the space discretization assuming that the successive IVP for the system of ODEs is solved exactly.

1.2 Outline of the rest of the paper

The paper is organized as follows. In Section 2 we introduce the model problem in a two dimensional domain: a system of two partial differential (reaction-diffusion) equations coupling two variables: the first variable lives only on the boundary of the domain, the second one is defined on the whole domain.

In Section 3 the finite element space discretization is applied to reduce the model problem to an IVP for a system of ODEs.

Section 4 is dedicated to the adaptive character of the method. In Section 4.1 we present the error estimation which is needed in driving an adaptivity process while the actual adaptive process is the subject of Section 4.2. Finally, Section 4.3 contains a series of remarks concerning special choices we have made within the error estimation and the adaptive strategy.

Section 5 contains our numerical experiments. In Section 5.1 we investigate the behavior of the (global) error estimator proposed in Section 4.1, while in Section 5.2 we test the local performance. Finally in Section 5.3 we examine the adaptive strategy proposed in Section 4.2.

The final section summarizes our findings and indicates possible future work.

2. A TWO DIMENSIONAL MODEL

For notational convenience and to keep the successive finite element implementation rather elementary, the exposition is limited here to a version of problem (1.1) in a two dimensional domain with two variables. The extensions of the method discussed in this paper to systems with more variables are straightforward while the higher dimensional case requires additional care.

Consider the reaction of two chemical species, the first, u_1, membrane-bound and the second, u_2, living in the cytosol. We model the process by a system of partial differential equations, in a two dimensional domain Ω – for detailed explanations of the model see [13],[25]. The species $u_1(x,y,t)$, which is confined to the cell membrane, is modeled by a concentration defined on the boundary of the domain, $\partial\Omega$. It is assumed to undergo diffusion as well as reaction:

$$\frac{\partial u_1}{\partial t} - \nabla \cdot (D_1 \nabla u_1) = R(u_1,u_2) \quad \text{for } (x,y) \in \partial\Omega, \quad t \in (0,T). \tag{2.1.a}$$

The process of the species $u_2(x,y,t)$, which is defined in the whole domain Ω, is described by

$$\frac{\partial u_2}{\partial t} - \nabla \cdot (D_2 \nabla u_2) = 0 \quad \text{for } (x,y) \in \Omega, \quad t \in (0,T). \tag{2.1.b}$$

For the mass balance of the interior species u_2, the reaction at the boundary represents a source/sink term. The corresponding boundary condition (BC) for species u_2 is then given by

$$D_2 \frac{\partial u_2}{\partial n} = -R(u_1,u_2) \quad n \text{ outward normal to } \partial\Omega. \tag{2.1.c}$$

In equations (2.1.a), (2.1.c), the term $R(u_1,u_2)$ defines the reaction rate. Note that since u_1 is a "line" concentration rather than a surface concentration, the rate $R(u_1,u_2)$ is also per unit length. In the above expression of $R(u_1,u_2)$, u_2 has to be interpreted as the value of the concentration at the location of the boundary. With some abuse of notation we could have written $R(u_1,u_2) = R(u_1(x,y,t),u_2(x,y,t))$ with $(x,y) \in \partial\Omega$.

To the above system initial conditions are provided:

$$u_1(x,y,0) = u_1^0(x,y) \text{ with } (x,y) \in \partial\Omega, \tag{2.1.d}$$
$$u_2(x,y,0) = u_2^0(x,y) \text{ with } (x,y) \in \Omega, \tag{2.1.e}$$

We note here that $u_2 \in \Omega$ belongs to $\mathbb{R}^2$ while, thinking to parametrize $\partial\Omega$ (for example with the arclength), we have $u_1 \in \partial\Omega \in \mathbb{R}^1$: the notation we use easily remembers such a situation (i.e. $u_i \in \mathbb{R}^i$, $i = 1,2$).

3. The finite element method of lines

In this section the finite element method of lines (FEMOL) approach is applied to obtain a numerical approximation of the solution of problem (2.1). With this approach the time dependent system of reaction-diffusion equations (2.1) is first semidiscretized in space by the Galerkin method. This results in a system of ordinary differential equations which has to be solved in time.

To this end, we define $V_1 = H^1(\partial\Omega)$ and $V_2 = H^1(\Omega)$ with $H^1(.)$ being the Sobolev space of functions u which are, together with the weak derivatives ∇u, square integrable. Then we construct the weak form of (2.1) in the standard way by multiplying (2.1.a) by a test function $v_1 \in V_1$ and (2.1.b) by a test function $v_2 \in V_2$ and integrating the results respectively over $\partial\Omega$ and Ω. Integrating the diffusive terms by parts, and using (2.1.c) we obtain the weak formulation of problem (2.1):

find, for all $t \in (0,T)$, $\quad u_1 \in V_1, \quad u_2 \in V_2$ such that:

$$\left(\frac{\partial u_1}{\partial t}, v_1\right)_1 + A_1(u_1,v_1) = (R(u_1,u_2),v_1)_1 \quad \text{for all } v_1 \in V_1, \tag{3.1.a}$$
$$\left(\frac{\partial u_2}{\partial t}, v_2\right)_2 + A_2(u_2,v_2) = (R(u_1,u_2),v_2)_1 \quad \text{for all } v_2 \in V_2. \tag{3.1.b}$$

Here, and in the following,

$$(f,g)_1 = (f,g)_{L_2(\partial\Omega)} = \int_{\partial\Omega} fg\,dxdy,$$
$$(f,g)_2 = (f,g)_{L_2(\Omega)} = \int_{\Omega} fg\,dxdy,$$
$$A_i(f,g) = (D_i \nabla f, \nabla g)_i \quad i = 1,2.$$

In the above expressions, ∇ has to be interpreted as the gradient operator in one or two dimensions. Note that the bilinear forms $A_i(.,.)$ define the energy norms of the problem: $A_i(f,f) = |||f|||_i^2$.

To simplify the notation, we introduce here the following convention: we indicate the solution of (3.1), containing both concentrations, with $u \in V = V_1 \times V_2$, i.e. $u = (u_1,u_2)$ and $u_1 \in V_1$, $u_2 \in V_2$.

Remark 3.1. *We observe that* (3.1) *can be interpreted as the weak formulation of a problem which is slightly different from* (2.1). *Consider equation* (2.1.b) *where the term* $\delta_S R(u_1,u_2)$ *is formally added to the right hand side. Here* δ_S *denotes the so called generalized delta function of a simple layer on* $S = \partial\Omega$ *(see [14]). Moreover, let the condition* (2.1.c) *be substituted with homogeneous Neumann boundary conditions. Then*

$$(\delta_S R(u_1,u_2),v_2)_2 = \int_{\Omega} \delta_S R(u_1,u_2) v_2\,dxdy = \int_{\partial\Omega} R(u_1,u_2) v_2\,dxdy = (R(u_1,u_2),v_2)_1$$

recovering once more (3.1.b).

From this prospective, problem (2.1) *can be seen as a diffusion reaction equation where a singular source, located at the boundary, is modeled by a generalized delta function – see also Remark 3.2 to be given below.*

The finite element approximation of problem (3.1) is obtained, with the standard procedure, by replacing V_1 and V_2 with finite dimensional subspaces $V_1^h \subset V_1$ and $V_2^h \subset V_2$. In constructing V_1^h and V_2^h we formally make use of two partitions $\mathcal{P}_1$ and $\mathcal{P}_2$ respectively of $\partial\Omega$ and Ω. We consider a decomposition $\mathcal{T}^h$ of Ω into triangles K with diameter h_K; we denote the size of the triangulation with $h = max_{K\in\mathcal{T}^h} h_K$. Here we assume that Ω has a polygon boundary and that the triangulation $\mathcal{T}^h$ has the standard properties used in the finite element method – see, e.g., [17]. For any triangle $K \in \mathcal{T}^h$ we denote with ∂K the set of its edges and with $\partial\mathcal{T}^h = \bigcup_{K\in\mathcal{T}^h} \partial K$. We then define the two partitions $\mathcal{P}_1$ and $\mathcal{P}_2$ as follow:

$$\mathcal{P}_1 = \mathcal{P}_1(\mathcal{T}^h) = \partial\mathcal{T}^h \cap \partial\Omega, \tag{3.2.a}$$

$$\mathcal{P}_2 = \mathcal{P}_2(\mathcal{T}^h) = \mathcal{T}^h. \tag{3.2.b}$$

Note that, even in the general case of systems with more variables, with the partitions defined above only one structure (corresponding to the underlying triangulation $\mathcal{T}^h$) is actually needed in the computations. The extension of the procedures, to be given in the following sections, to the case of different partitions for different variables requires additional considerations.

Here and in the following, we reserve the letter K to indicate a triangle in $\mathcal{T}^h$ while we will use the letter E to indicate an element of $\mathcal{P}_i$ independently if it is an interval ($i = 1$) or a triangle ($i = 2$).

The finite dimensional spaces V_1^h and V_2^h are finally defined below:

$$V_1^h = V_1^h(\mathcal{T}^h) = \{v \in \mathscr{C}(\partial\Omega); \quad v|_E \in \Pi_p(E) \text{ for all } E \in \mathcal{P}_1(\mathcal{T}^h)\}, \tag{3.3.a}$$

$$V_2^h = V_2^h(\mathcal{T}^h) = \{v \in \mathscr{C}(\Omega); \quad v|_E \in \Pi_q(E) \text{ for all } E \in \mathcal{P}_2(\mathcal{T}^h)\}. \tag{3.3.b}$$

Above $\mathscr{C}(\Omega)$ and $\mathscr{C}(\partial\Omega)$ are respectively the spaces of the continuous functions defined on Ω and $\partial\Omega$; $\Pi_r(E)$ is the space of all polynomials of degree $\leq r$ defined on an element E.

Based on the weak formulation (3.1), and with the help of definition (3.3), we formulate below the finite element problem by approximating for all $t \in (0,T)$, $u_1(t)$ by $u_1^h(t)$ in the finite dimensional space $V_1^h \subset V_1$ and $u_2(t)$ by $u_2^h(t)$ in the finite dimensional space $V_2^h \subset V_2$.
Given a triangulation $\mathcal{T}^h$

$$\text{find, for all } t \in (0,T), \quad u_1^h \in V_1^h, \quad u_2^h \in V_2^h \text{ such that:}$$

$$\left(\frac{\partial u_1^h}{\partial t}, v_1^h\right)_1 + A_1(u_1^h, v_1^h) = (R^h, v_1^h)_1 \quad \text{for all } v_1^h \in V_1^h \tag{3.4.a}$$

$$\left(\frac{\partial u_2^h}{\partial t}, v_2^h\right)_2 + A_2(u_2^h, v_2^h) = (R^h, v_2^h)_1 \quad \text{for all } v_2^h \in V_2^h. \tag{3.4.b}$$

Here $R^h = R^h(u_1^h, u_2^h)$ represents an approximation of $R(u_1, u_2)$ on V_1^h.

Similar to what we have already done for system (2.1), we denote the solution of (3.4) with $u^h = (u_1^h, u_2^h)$ and we write $u^h \in V^h$, to indicate that $u_1^h \in V_1^h$, $u_2^h \in V_2^h$.

Remark 3.2. *In connection with Remark 3.1, the right hand side of equation* (3.4.b) *can be seen as the numerical implementation of the singular source term (singular in the sense that within the spatial domain, the source is defined by a generalized delta function on a lower dimension). Usually singular source terms in differential equations pose several difficulties for its numerical approximation. For example the lack of smoothness of the solution may cause order reduction – see, e.g, [4] and [30]. With the situation at hand, it is of fundamental importance to note that the singular source will always be located at nodal points (at the boundary) avoiding in such a way many of the difficulties mentioned above. Much more attention would have been needed if the reaction among the two species were located in a lower dimensional surface inside the domain Ω (such situation, e.g., appears when modeling reactions at the DNA, reactions at the membrane of compartments in the cytoplasm of eukaryotic cells and flame propagation).*

Let $\{\varphi_{i,1}, ..., \varphi_{i,DOF_i}\}$ be a base of V_i^h (where DOF stands for degrees of freedom). For example, assume $\varphi_{1,j}$, $j = 1, ..., DOF_1$ are the Lagrange polynomials of degree p defined on the DOF_1 nodal points associated with the partition $\mathcal{P}_1$ and $\varphi_{2,j}$, $j = 1, ..., DOF_2$ the Lagrange polynomials of degree

q defined on the DOF_2 nodal points associated with the partition $\mathcal{P}_2$. Then $u_i^h = \sum_{j=1}^{DOF_i} U_{i,j}(t)\varphi_{i,j}$ where $U_1(t) = (U_{1,1}(t), ..., U_{1,DOF_1}(t))$ and $U_2(t) = (U_{2,1}(t), ..., U_{2,DOF_2}(t))$ are the vectors of the nodal values of u_1^h and u_2^h respectively.

Taking into consideration the fact that (3.4) has to be satisfied for all $v_1^h \in V_1^h$ and all $v_2^h \in V_2^h$, it is clear that equations (3.4) are equivalent to requiring that the $(DOF_1 + DOF_2)$-dimensional vector of the nodal values $U(t) = (U_1(t), U_2(t))$ satisfies the following IVP for system of ordinary differential equations

$$M\frac{d}{dt}U(t) + SU(t) = F(U(t)), \tag{3.5.a}$$

$$U(0) = U_0. \tag{3.5.b}$$

In equation (3.5.a) M and S are the so called mass and stiffness matrices which are symmetric and, respectively, positive definite and nonnegative. With the situation at hand (without special reordering of the nodal points), the matrices M and S are block diagonal matrices of the form

$$M = \begin{pmatrix} M_1 & 0 \\ 0 & M_2 \end{pmatrix}, \quad S = \begin{pmatrix} S_1 & 0 \\ 0 & S_2 \end{pmatrix} \tag{3.6.a}$$

where

$$(M_i)_{l,m} = (\varphi_{i,l}, \varphi_{i,m})_i, \quad i = 1, 2. \tag{3.6.b}$$

$$(S_i)_{l,m} = A_i(\varphi_{i,l}, \varphi_{i,m}), \quad i = 1, 2. \tag{3.6.c}$$

The function F from $\mathbb{R}^{DOF_1+DOF_2}$ into itself takes care of the reaction terms appearing in equations (3.4). Finally, U_0 is the vector of the nodal values of the approximation in the finite element spaces V_1^h and V_2^h of the initial conditions (2.1.d) and (2.1.e).

The FEMOL approximation u^h, solution of (3.4), is obtained solving numerically equation (3.5) with, e.g., a step-by-step method. With this approach, each step starts from a given approximation U^{n-1} of $U(t)$ at a point $t = t_{n-1} \geq 0$. A stepsize $\Delta t > 0$ is selected and t_n is set equal to $t_{n-1} + \Delta t$. An approximation U^n of $U(t_n)$ is then computed from U^{n-1}. The result of this step, U^n, is then the starting value for the next step.

In order to achieve a prescribed level of accuracy, different triangulations $\mathcal{T}^h$ (and consequently different spaces $V_1^h(\mathcal{T}^h)$ and $V_2^h(\mathcal{T}^h)$) might be used at different time level. The triangulation $\mathcal{T}^h$ will be automatically adapted during the time integration according to an estimation of the error of the spatial discretization. The error estimation and the adaptive process are described in the next section.

4. Error estimators and an adaptive process

In this section we apply (and modify) the adaptive finite element method of lines for parabolic equations of the reaction-diffusion type proposed by Bieterman and Babuška in [12]. In such an approach the local mesh size is automatically adapted according to an explicit estimation of the space discretization error.

We discuss in the next section the approximation of the error. The adaptive method is presented in Section 4.2.

4.1 Error estimators

With the notation of Section 3, let $u^h = (u_1^h, u_2^h)$ $(u_i^h \in V_i^h(\mathcal{T}^h),\ i = 1, 2)$ be the solution of (3.4) which approximates $u = (u_1, u_2)$ $(u_i \in V_i,\ i = 1, 2)$, the solution of problem (3.1). Moreover, according to the definitions (3.2), given an element E in a partition $\mathcal{P}_i(\mathcal{T}^h)$, we indicate with h_E the length of the interval E (if $i = 1$) or the diameter of the triangle E (if $i = 2$). In the following we define the (global) error estimators $\mathcal{E}_i(u^h(t))$ which approximate the energy norm of the error $|||e_i(t)|||_i = |||u_i(t) - u_i^h|||_i$ for $i = 1, 2$.

We start defining the (global) error estimator $\mathcal{E}_1(u^h(t))$ by

$$\mathcal{E}_1(u^h(t)) = \left\{ \sum_{E \in \mathcal{P}_1} \eta_{1,E}^2(u^h(t)) \right\}^{1/2}. \tag{4.1.a}$$

Here $\eta^2_{1,E}(u^h(t))$ is the (local) error indicator (for the variable u^h_1) on the (interval) element $E \in \mathcal{P}_1$ defined by

$$\eta^2_{1,E}(u^h(t)) = c_1^{int} h_E^2 ||r_1^{int}(u^h(t))||^2_{L_2(E)} \tag{4.1.b}$$

where we have used the standard L_2-norm: $\|u\|^2_{L_2(\circ)} = \int_\circ |u|^2$. The quantity c_1^{int} is a given constant the choice of which will be discussed in Section 4.3 (remark (EE2)). The quantity $r_1^{int}(u^h(t))$ is the internal residual (for the variable u^h_1) defined by

$$r_1^{int}(u^h(t)) = \frac{\partial u^h_1}{\partial t} - \nabla \cdot (D_1 \nabla u^h_1) + R(u^h_1, u^h_2). \tag{4.1.c}$$

The definition of the (global) error estimator $\mathcal{E}_2(u^h(t))$, although it is similar to $\mathcal{E}_1(u^h(t))$, is more complex and it involves an additional term related to the gradient of u^h_2 at the boundary ∂E of any triangular element E.

We define

$$\mathcal{E}_2(u^h(t)) = \left\{ \sum_{E \in \mathcal{P}_2} \eta^2_{2,E}(u^h(t)) \right\}^{1/2}. \tag{4.2.a}$$

Here $\eta^2_{2,E}(u^h(t))$ is the (local) error indicator (for the variable u^h_2) on the (triangular) element $E \in \mathcal{P}_2$ defined by

$$\eta^2_{2,E}(u^h(t)) = c_2^{int} h_E^2 ||r_2^{int}(u^h(t))||^2_{L_2(E)} + c_2^{bou} h_E ||r_2^{bou}(u^h(t))||_{L_2(\partial E)}. \tag{4.2.b}$$

Above c_2^{int} and c_2^{bou} are given constant (the choice of which will be discussed in Section 4.3, remark (EE2)) and the quantities $r_2^{int}(u^h(t))$, $r_2^{bou}(u^h(t))$ are respectively the internal and the boundary residual (for the variable u^h_2) defined, on each element, by

$$r_2^{int}(u^h(t)) = \frac{\partial u^h_2}{\partial t} - \nabla \cdot (D_2 \nabla u^h_2); \tag{4.2.c}$$

$$r_2^{bou}(u^h(t)) = \begin{cases} R(u^h_1, u^h_2) - \frac{\partial u^h_2}{\partial n} & \text{for } \partial E \cap \partial\Omega, \\ -\frac{1}{2} [\![\frac{\partial u^h_2}{\partial n}]\!]_\gamma & \text{for } \gamma \in \partial E,\ \gamma \notin \partial\Omega. \end{cases} \tag{4.2.d}$$

In equation (4.2.d) the quantity $[\![\frac{\partial u^h_2}{\partial n}]\!]_\gamma$ denotes the jump of the gradient of u^h_2 among two triangles of the partition $\mathcal{P}_2$ sharing the same internal edge γ.

4.2 An adaptive process

In the adaptive process given below, the error estimators $\mathcal{E}_i(u^h)$ and the error indicators $\eta^2_{i,E}(u^h(t))$ (defined respectively in (4.1) (4.2)) are computed at each time t in a set of initially given times $\{t_n,\ n = 1, 2, ..., N\} \subseteq (0, T)$. Then, depending on the computed values $\mathcal{E}_i(u^h)$ and $\eta^2_{i,E}(u^h(t))$, a regridding occurs at time $\{t_{n_k},\ n_k \subseteq (1, 2, ..., N)\}$.

To keep the presentation of the adaptive algorithm sufficiently concise, we will use the following notation.

(Proj) Given two triangulations $\mathcal{T}^h_{old}$ and $\mathcal{T}^h_{new}$ and u^h_{old} belonging to the finite element space $V^h(\mathcal{T}^h_{old})$, we indicate with $\mathsf{Proj}(u^h_{old}, \mathcal{T}^h_{new})$ the function that project the function u^h_{old} on the new finite element space $V^h(\mathcal{T}^h_{new})$.

(ODESolve) Given a triangulation $\mathcal{T}^h$, a function u^h belonging to the finite element space $V^h(\mathcal{T}^h)$ and a time step Δt, we indicate with $\mathsf{ODESolve}(u^h, \Delta t)$ the function returning the solution, after time Δt, of the semidiscrete system (3.4). This solution is computed solving the initial value problem (3.5) where the initial condition U_0 is the vector of nodal values of u^h.

(Regrid) Let $\mathcal{E}_i(u^h)$ and $\eta_{i,E}(u^h)$ be the (global) error estimators and the (local) error indicators defined in (4.1), (4.2). We indicate with $\mathsf{Regrid}(\mathcal{E}_i(u^h), \eta_{i,E}(u^h))$ the boolean function which is true if regridding is needed and false otherwise.

(Adapt) Given a triangulation $\mathcal{T}^h$, the (global) error estimators $\mathcal{E}_i(u^h)$ and the (local) error indicators $\eta_{i,E}(u^h)$, we indicate with $\mathsf{Adapt}(\mathcal{T}^h, \mathcal{E}_i(u^h), \eta_{i,E}(u^h))$ the function returning the adapted triangulation according to the information in $\mathcal{E}_i(u^h)$ and $\eta_{i,E}(u^h)$.

Schematically the algorithm is as follows:

Let the time partition $\{0 = t_0, t_1, ..., t_N = T\}$ be given, $\mathcal{T}_0^h$ an initial triangulation and let $u^h(t_0)$ be an initial value in $V^h(\mathcal{T}_0^h)$.
$n = 1$
while $n \leq N$
  $\mathcal{T}^* = \mathcal{T}_{Base}$
  Modflag $= 1$
  while Modflag $= 1$
    $u^*(t_{n-1}) = \mathsf{Proj}(u^h(t_{n-1}), \mathcal{T}^*)$
    $u^*(t_n) = \mathsf{ODESolve}(u^*(t_{n-1}), t_n - t_{n-1})$
    if $\mathsf{Regrid}(\mathcal{E}_i(u^*(t_n)), \eta_{i,E}(u^*(t_n)))$
      $\mathcal{T}^* = \mathsf{Adapt}(\mathcal{T}^*, \mathcal{E}_i(u^*(t_n)), \eta_{i,E}(u^*(t_n)))$
    else
      $u^h(t_{n-1}) = u^h(t_n) = u^*(t_n)$
      $\mathcal{T}_{n-1}^h = \mathcal{T}_n^h = \mathcal{T}^*$
      $n = n + 1$
      Modflag $= 0$
    end
  end
end

Starting from the given initial condition $u^h(t_0) \in V^h(\mathcal{T}_0^h)$ the algorithm produces, for each time level $\{t_n,\ n = 1, 2, ..., N\} \subseteq (0, T)$ a triangulation $\mathcal{T}_n^h$, and the corresponding solution $u^h(t_n) \in V^h(\mathcal{T}_n^h)$, so that the (global) error estimators $\mathcal{E}_i(u^h(t_n))$ and the (local) error indicators $\eta_{i,E}(u^h(t_n))$ satisfy certain requirements (i.e. $\mathsf{Regrid}(\mathcal{E}_i(u^h(t_n)), \eta_{i,E}(u^h(t_n)))$ is false).

At each time level t_n, the determination of the triangulation $\mathcal{T}_n^h$ is done modifying (if necessary) a fixed basic triangulation $\mathcal{T}_{Base}$ which is the coarsest triangulation that can be used – see remark (AA1) to be given below. Starting from $\mathcal{T}_{Base}$ the algorithm produces a sequence of triangulations $\mathcal{T}^*$ (see (AA3), (AA4)) until no further modifications are needed and $\mathcal{T}^*$ meets the requirements (see (AA2)). Then $\mathcal{T}_n^h$ is set equal to $\mathcal{T}^*$ and the search for the new triangulation for the next time level starts (or the algorithm stops because the final time $t_N = T$ is reached).

4.3 A series of remarks

In the following series of remarks we clarify the special choices we have made within the error estimation of Section 4.1 and the adaptive algorithm of Section 4.2 . The first two points concern the error estimation (indicated with EE); the last six points are related to the adaptive algorithm (indicated with AA).

(EE1) In formula (4.2.d) we replaced, in the boundary condition, the unknowns u_1, u_2 with u_1^h, u_2^h, i.e., we have written $R(u_1^h, u_2^h) - \frac{\partial u_2^h}{\partial n}$ instead of $R(u_1, u_2) - \frac{\partial u_2^h}{\partial n}$. We note here that, with the last modification, we obtain an error estimator $\mathcal{E}_2(u^h(t))$ which estimates problem (2.1) where (2.1.c) is replaced by $D_2 \frac{\partial u_2}{\partial n} = -R(u_1^h, u_2^h)$ rather than the original one. This fact will have an important role in the explanation of the results given in Section 5.2.

(EE2) In order to make (4.1) and (4.2) fully computable a-posteriori error estimates, we have to decide upon the constants c_1^{int}, c_2^{int}, c_2^{bou}. In both formulas the constants depend only on the regularity of the respective partitions $\mathcal{P}_1(\mathcal{T}^h)$ and $\mathcal{P}_2(\mathcal{T}^h)$ (and eventually on some equation parameters). Because in the numerical studies, to be given below, piecewise linear elements are used, we have fixed $c_1^{int} = \frac{1}{12D_1}$; see, e.g., [6],[12]).

The choice of the other two constants (c_2^{int}, c_2^{bou}) is, on the contrary, less clear. For a 2-dimensional domain Ω we have the unfortunate situation that $H^1(\Omega) \not\subseteq \mathscr{C}(\Omega)$ and the Lagrange interpolation, in deriving the error estimation, cannot be used. Moreover, the additional contribution of the jumps of the gradient of u_2^h between two element can not be neglected.

It is well known that those constants depend on the shape of the triangular elements but usually they are not calculated. In particular we observe that the choice of the constants weights the importance of the contributions of the internal residual $r_2^{int}(u^h(t))$ and the boundary residual $r_2^{bou}(u^h(t))$. Without too much knowledge it seems natural to opt for equal constants. Actually, as we will see in Section 5.2, this appears not to be the best choice.

Lower and upper estimates for the constants that depend on the edges of the triangles are given in [5]. However, such estimates (for linear elements) yield equal constants c_2^{int}, c_2^{bou}. Following Carstensen and Funken [15] – where the derivation of the two constants is done making use of the Clément interpolation operator [18] – we set $c_2^{bou} = 12 \cdot c_2^{int}$. The exact value of the two constants is of less importance (at least when driving adaptivity). Because we always consider convex domains and triangulations which are quite regular – in the sense that the minimal angle of any triangle varies in a small range – we fix $c_2^{int} = \frac{1}{12D_2}$ and consequently $c_2^{bou} = \frac{1}{D_2}$.

We note here that for higher order elements different constants might be needed.

(AA1) To simplify the data structure which is used in the actual implementation of the finite element method, we have replaced the more natural assignment $\mathcal{T}^* = \mathcal{T}^h_{n-1}$ with $\mathcal{T}^* = \mathcal{T}_{Base}$ where $\mathcal{T}_{Base}$ is the coarsest triangulation that can be used. This is not an optimal choice but with this replacement we essentially do not need a coarsening routine which is usually very demanding from the implementational structures point of view: starting with a triangulation equal to $\mathcal{T}_{Base}$, we just refine it up to the point that a certain accuracy is achieved – see (AA2) and (AA3).

(AA2) Decisions concerning mesh modifications are usually based on achieving

$$C_{low}\, Tol_i \leq \mathcal{E}_i(u^h(t)) \leq C_{up}\, Tol_i \tag{4.3}$$

for a fixed tolerance Tol_i and given constants C_{low} and C_{up} (e.g. $C_{low} = 1/2$ and $C_{up} = 2$). As an immediate consequence of (AA1), we can essentially avoid to consider the left hand side of (4.3) simply requiring the (global) error estimators $\mathcal{E}_i(u^h(t))$ to be below given tolerances.

The actual test that is used in the function Regrid is the standard combination of absolute and relative errors

$$\mathcal{E}_i(u^h(t)) \leq Tol_i^A + Tol_i^R \;|||\, u_i^h(t)\,|||_i \tag{4.4}$$

for each variable u_i, $i = 1, 2$. Here Tol_i^A and Tol_i^R indicate the absolute and relative error tolerances. Since we attempt to achieve an equal error for the boundary and the internal species, we set $Tol_1^\circ = \left(\frac{Ar(\Omega)}{Le(\partial\Omega)}\right)^{1/2} Tol_2^\circ$ ($\circ = A, R$) where $Ar(\Omega)$ and $Le(\partial\Omega)$ are respectively the area of the two dimensional domain Ω and the length of its boundary.

(AA3) The regridding of the triangulation $\mathcal{T}^*$ is performed in the function Adapt. According to the indications returned by the function Regrid, the function Adapt performs a refinement of the underlying triangulation $\mathcal{T}^*$.

Several adaptive strategies are proposed in the literature that give criteria to decide which elements should be refined. All strategies are based on the idea that a partition is optimal when the error is equal for all elements. Accordingly, an element E which has the indicator error $\eta_{i,E}$ exceeding a certain threshold will be marked for refinement. For the actual choice of the refinement strategy see point (AA4).

Let $E2ref_i = \left\{ E_j \,|\, E_j \in \mathcal{P}_i(\mathcal{T}^*),\, j = 1, \ldots N_i^{ref} \right\}$ be the sets of elements marked for refinement for each of the two variables u_i^h, $i = 1, 2$. We stress once more that an element $E \in \mathcal{P}_1(\mathcal{T}^*)$ is an interval while an element $E \in \mathcal{P}_2(\mathcal{T}^*)$ is a triangle. Then a triangle $K \in \mathcal{T}^*$ is refined if K is an element of $E2ref_2$ or if (at least) one of its edges is in $E2ref_1$.

The refinement algorithm will be *regular* or *longest*: with the *regular* refinement the triangle $K \in \mathcal{T}^*$ is divided into four triangles with the same shape, while with the *longest* refinement the longest edge of the triangle is bisected. Some extra triangles may be also refined in order to avoid hanging nodes or triangles which are too stretched.

(AA4) The sets $E2ref_i$ are defined by the computed values $\mathcal{E}_i$ and $\eta_{i,E}$. Among the variety of refinement strategies available in the literature, we have implemented the following 3 possibilities:

(i) *Maximum strategy* [7]: given $\theta \in [0,1]$ then:

$$E \in E2ref_i \text{ iff } \eta_{i,E} \geq \theta \cdot \max_{E \in \mathcal{P}_i} \eta_{i,E}.$$

A small value of θ leads to a large number of elements marked for refinement and to an almost uniform mesh, while a large value of θ leads to an optimal graded mesh (but more trials for $\mathcal{T}^*$ until the error tolerance is reached).

(ii) *Equidistribution strategy* [22]: let $N_{\mathcal{P}_i}$ be the number of elements E of the partition $\mathcal{P}_i$ and Tol_i the error tolerance required. In the ideal situation where the error is equidistributed over the domain, i.e. $\eta_{i,E} = \eta_i$ for all $E \in \mathcal{P}_i$, we have $\eta_i \sqrt{N_{\mathcal{P}_i}} = Tol_i$. One can aim for the equidistribution of the error defining the sets $E2ref_i$ by

$$E \in E2ref_i \text{ iff } \eta_{i,E} \geq \frac{\theta \cdot Tol_i}{\sqrt{N_i^{\mathcal{P}}}}$$

where the parameter $\theta \in [0,1]$ is introduced to make the procedure more robust.

(iii) *Robust error reduction strategy* [20]: let $\theta \in [0,1]$ be given. Then $E2ref_i$ is the minimum set such that

$$\sum_{E \in E2ref_i} \eta_{i,E}^2 \geq (1-\theta)^2 \mathcal{E}_i^2.$$

With this strategy the subset $E2ref_i$ of the partition $\mathcal{P}_i$ is defined to reduce, proportionally to θ, the global error estimators $\mathcal{E}_i$. Once again, a small value of θ leads to a large number of elements marked for refinement and to an almost uniform mesh, while a large value of θ leads to an optimal graded mesh (but more trials for $\mathcal{T}^*$ until the error tolerance is reached).

(AA5) To obtain an approximation $u^h_{new} \in V^h(\mathcal{T}^h_{new})$ to $u^h_{old} \in V^h(\mathcal{T}^h_{old})$ we define the function Proj to be an interpolation at nodal points. Although an L_2-projection would possibly be more appropriate, our choice is cheaper, simpler to be implemented and its employment does not interfere with the overall performance of the adaptive procedure as long as the solutions are sufficiently smooth or not too crude error tolerances are required – see [9] for related considerations.

(AA6) The call of the function ODESolve$(u^h, \Delta t)$ computes the solution after time Δt of the IVP (3.5.a) (where the initial condition U_0 is the vector of nodal values of u^h) using a variable-step explicit fourth-order Runge-Kutta method. Typically many time steps are taken for the integration of the ODE (3.5) during the time interval Δt.

To be able to compute the error estimation defined in (4.1), (4.2) (and especially the time derivatives appearing in (4.1.c) and (4.2.c)) the ODESolve function not only returns the solution after time Δt, let say $u^h_{\Delta t}$, but also a second solution, let say u^h_ε, after time $(1-\varepsilon)\Delta t$. Then we can easily approximate the time derivative $\frac{\partial u^h}{\partial t}$ with $\frac{u^h_{\Delta t} - u^h_\varepsilon}{\varepsilon \Delta t}$.

We note here that the matrices M and S, appearing in equation (3.5), have to be updated after each modification of the triangulation $\mathcal{T}^h$. The matrices after a modification are clearly related to the old ones but, to simplify the implementation, no advantage is taken here of this fact and all matrices entries are recomputed after each mesh refinement.

In order to isolate the space discretization error, in all the computations, the ODE system is essentially solved exactly – it is computed by using a very small error tolerance so that the errors due to the space discretization dominate those due to the time integration. The main goal here is to examine more carefully the performance of the error estimation and the successive adaptive strategy for the system of reaction-diffusion equations (2.1) coupling chemical species living in different domains. No consideration is given here either to the amount of computational work (and the resulting computational time) or to the question of how best to balance the space and time discretization error – for the last problem we refer to [26].

5. Numerical experiments

In this section we test the adaptive finite element method of line (FEMOL) presented in Section 3 and Section 4.

The most important components of the adaptive strategy are the a-posteriori (global) error estimators $\mathcal{E}_i$ and the (local) error indicators $\eta_{i,E}$ on which all the decisions of *when* and *where* to modify the underlying triangulation are based.

In order to assess the performance of the adaptive FEMOL we focus our attention on three different aspects: the behavior of the global estimators $\mathcal{E}_i$ (defined in (4.1.a), (4.2.a)), the behavior of the local error indicators $\eta_{i,E}$ (defined in (4.1.b), (4.2.b)) and finally the ability of the adaptive strategy to change the triangulation $\mathcal{T}^h$ attempting to obtain at any time a solution $u^h(t) \in V^h(\mathcal{T}^h)$ which realizes a good compromise between high accuracy and low computational complexity.

The rest of this section is organized as follow. In Section 5.1 we compare the (global) error estimators $\mathcal{E}_i$ with the energy norm of the error $|||e_i(t)||| = |||u_i(t) - u_i^h(t)|||$. We will see that for a triangulation $\mathcal{T}^h$ with different mesh size h and at different times, the (global) error estimators $\mathcal{E}_i$ adequately reproduce the behavior of $|||e_i(t)|||$. This guarantees a good selection of points in time *when* regridding is necessary, i.e. on which of the time-points $\{0 = t_0, t_1, ..., t_N = T\}$ the regridding is needed.

The second even more important question on *where* to modify the triangulation is the material of Section 5.2. Here we investigate the ability of the (local) error indicators $\eta_{i,E}$ to detect correctly from which part of the domain the major problems come.

In the last Section 5.3 we test the performance of the adaptive strategy to automatically find an optimal triangulation.

In the coming sections we refer to a system of reaction-diffusion equations of the form (2.1) where the reaction term, defined by

$$R(u_1, u_2) = k_{12}u_1 - k_{21}u_2$$

models the chemical equilibrium of u_1 and u_2 at the boundary of the domain

$$u_1 \underset{k_{21}}{\overset{k_{12}}{\leftrightarrows}} u_2.$$

In order to simplify the convergence studies to be given in Section 5.1 and to avoid poor regularity of the solution due to the influence of the domain, we confine our studied on the square with vertices in $(-1,-1), (1,-1), (1,1), (-1,1)$. Note that it is well known that, already for elliptic problems, the regularity of a solution on a polygon domain depends on the maximal internal angle, see, e.g., [19].

We finally mention here that, for the results contained in the following sections, the integrals, as well as the L_2 norms and the energy norms, are computed using Gauss-Legendre quadrature rules with appropriate order so that all the mentioned quantities are calculated exactly (up to machine precision). The actual implementation is done in MATLAB.

5.1 The performance of the global error estimators

In this section we asses the performance of the global error estimators $\mathcal{E}_i$ (Section 4.1) when solving problem (2.1) with the finite element method of lines (Section 3).

For $t \to \infty$ the solution $u = (u_1, u_2)$ of problem (2.1) approaches exponentially fast the steady state

$$u_1^\infty = k_{21} \frac{\int_{\partial\Omega} u_1^0 + \int_\Omega u_2^0}{k_{21} \cdot Le(\partial\Omega) + k_{12} \cdot Ar(\Omega)} \tag{5.1.a}$$

$$u_2^\infty = k_{12} \frac{\int_{\partial\Omega} u_1^0 + \int_\Omega u_2^0}{k_{21} \cdot Le(\partial\Omega) + k_{12} \cdot Ar(\Omega)} \tag{5.1.b}$$

Once more we have indicated with $Ar(\Omega)$ the area of the domain Ω and with $Le(\partial\Omega)$ the length of its boundary. We have fixed the initial conditions by $u_1^0 = 1$ on $\partial\Omega$ and $u_2^0 = 0$ on Ω, the diffusion coefficients $D_1 = 0.1$, $D_2 = 1$ and the chemical reaction coefficients by $k_{12} = k_{21} = 1$. Furthermore, since we are interested in the transient behavior of the problem, we consider a finite time interval $[0, T]$.

Due to the the initial conditions which are not in equilibrium, species u_2 develops, at the beginning, steep gradients at the boundary. Moreover, due to the geometry of the problem, both species u_1

and u_2 develop peaks at the four corners – the reader can have an idea of the solution at increasing time looking at Figures 3 and 4.

Problem (3.4) (with the reaction term, initial conditions and parameters given above) is solved with linear elements ($p = q = 1$) on uniform triangulations $\mathcal{T}^h$ of size $h = 2^{1-n_{ref}}$ for increasing number of (regular) refinements $n_{ref} = 0, 1, 2, ..., 6$ – the initial triangulation $\mathcal{T}^h$ with $h = 2$ consists of four equal isosceles right triangles generated connecting the four corners with the center of the square. Note that the choice of $p = q$ is particularly convenient in the light of the following fact: let $v \in V_2^h$ and $\gamma \in \mathcal{P}_1(\mathcal{T}^h)$ be an edge of a triangle element $E \in \mathcal{P}_2(\mathcal{T}^h)$, if $p = q$, we have $v|_\gamma \in V_1^h$ – see definitions (3.2).

Figures 1, 2 and Tables 1, 2 and 3 summarize the results. In the figures we compare the convergence of the errors and the estimations. The exact solution $u(t) = (u_1(t), u_2(t))$ was taken to be the numerical solution computed with 7 refinements and very accurate time integration. We recall from Section 3 that the energy norms $|||.|||_i$ are L_2 (weighted) gradient norms and, from the standard theory of finite element method, the errors (in such a norm) are expected to converge to zero with order 1 for decreasing space grid size.

The tables collect the values of the effectivity indices $\Theta_i^h(t)$ $(i = 1, 2)$ defined by

$$\Theta_i^h(t) = \frac{\mathcal{E}_i(u^h(t))}{|||u_i(t) - u_i^h(t)|||_i}$$

A major property demanded of all successful error estimators is that positive constants C_i^{low} and C_i^{up} exist such that $C_1^{low} \leq \Theta_i^h(t) \leq C_i^{up}$ for all time $t \in [0, T]$. Then the error estimators $\mathcal{E}_i(u^h(t))$ tend to zero at the same rate as the energy norms of the errors $|||e_i(t)|||_i$. Naturally, one hopes that $\Theta_i^h(t)$ close unity can be obtained but effectivity indices of 2-5 or even higher are regarded as acceptable in many applications.

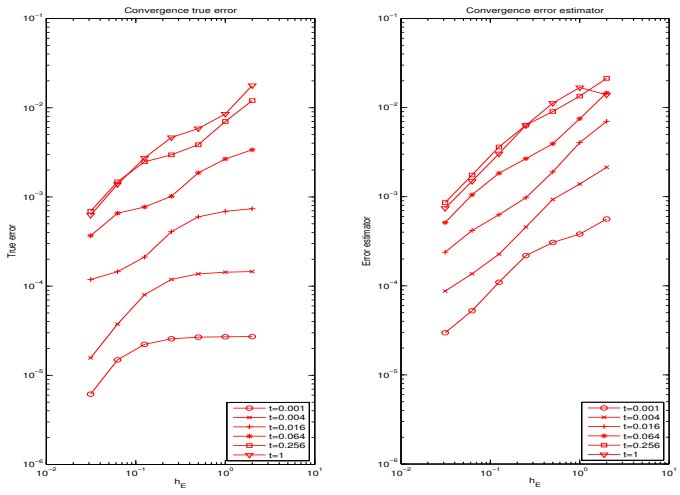

Figure 1: The error (left) and the error estimator $\mathcal{E}_1$ (right)

Figure 1 shows, for increasing time and decreasing grid size (i.e. increasing number of refinements), the behavior of the error for species u_1 and the behavior of the (global) estimator $\mathcal{E}_1$. The first quantity shows a slow convergence behavior while the second one exhibits a rather clear order 1 convergence to zero. Note that, for a specific triangulation, the error increases with time. This fact is related to the accentuation of the peaks at the four corners when time evolves – see Figure 3 (left).

The quality of the estimator can be seen in Table 1 where we have collected the value of the effectivity index $\Theta_1^h(t)$ for the corresponding time and number of refinements of Figure 1. Note that not only the effectivity index remains reasonable bounded but, in general, it also becomes closer to 1 when the number of refinements increases – the increasing values corresponding to 6 refinements have to be attributed to the influence of the reference solution which has just one extra refinement

	$n_{ref}=0$	$n_{ref}=1$	$n_{ref}=2$	$n_{ref}=3$	$n_{ref}=4$	$n_{ref}=5$	$n_{ref}=6$
$t=0.001$	20.7	14.1	11.4	8.5	4.9	3.5	4.8
$t=0.004$	14.7	9.7	6.8	3.8	2.8	3.6	5.6
$t=0.016$	9.5	5.9	3.2	2.4	3.0	2.9	2.0
$t=0.064$	4.3	2.8	2.1	2.6	2.4	1.6	1.4
$t=0.256$	1.8	1.9	2.3	2.1	1.5	1.2	1.2
$t=1.000$	0.8	2.0	1.9	1.4	1.1	1.0	1.2

Table 1: The effectivity index $\Theta_1^h(t)$

($n_{ref}=7$). Observe that the quantity $\Theta_1^h(t)$ decreases also when time increases. In fact (see Figure 3), the solution u_1^h, which initially develops sharp peaks of increasing height, approaching the steady state, becomes smoother. Clearly the estimation of the spatial error is more accurate when the solution is smooth.

A similar analysis is done for species u_2. In Figure 2 we plot the energy norm of the error and two error estimators of the type $\mathcal{E}_2$. According to remark (EE2), we have fixed the constants (appearing in (4.2.b)) to $c_2^{int}=\frac{1}{12D_2}$ and $c_2^{bou}=\frac{1}{D_2}$ for the first error estimator (central picture). The second one (right picture) is obtained using $c_2^{int}=c_2^{bou}=\frac{1}{12D_2}$. Clearly for species u_2 the theoretical

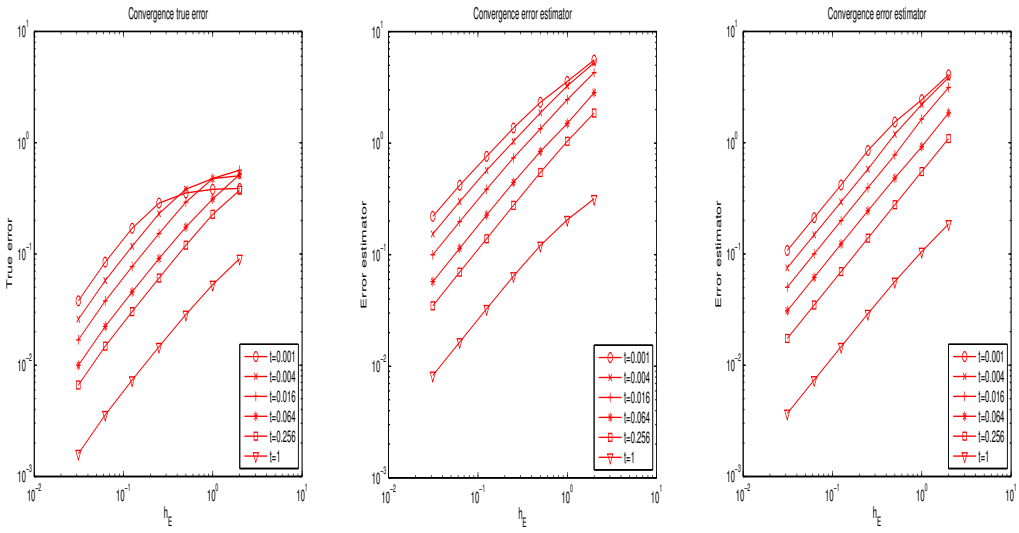

Figure 2: The error (left) and the error estimator $\mathcal{E}_2$ with $c_2^{int}=12\cdot c_2^{bou}$ (center) and with $c_2^{int}=c_2^{bou}$ (right)

first order convergence of the energy error is recovered. The same behavior is shown for the error estimators. Observe that in contrast to u_1, the error and the error estimator of u_2 essentially always decrease with time – only for very coarse triangulations and times close to zero the error grows.

The quality of the error estimators can be seen in Table 2 and Table 3 where, similarly to what we have done for u_1, we have collected the values of the effectivity index $\Theta_2^h(t)$. Note that the values of $\Theta_2(t)$ in Table 3 (corresponding to the case $c_2^{bou}=c_2^{int}$) are closer to 1 than the values of Table 2 (corresponding to the case $c_2^{bou}=12c_2^{int}$). One may thus be tempted to conclude that $c_2^{bou}=c_2^{int}$ is a better choice than $c_2^{bou}=12\cdot c_2^{int}$. As we will see in the next section such comparison is quite misleading: it is a global consideration which is not valid at the local level.

For further reference we note from Figure 2 that for having an error estimator $\mathcal{E}_2$ (with $c_2^{bou}=12c_2^{int}$) below $2\cdot 10^{-1}$ at all times, we need 6 uniform refinements corresponding to a triangulation $\mathcal{T}^h$ with $4^7=16384$ triangles.

	$n_{ref}=0$	$n_{ref}=1$	$n_{ref}=2$	$n_{ref}=3$	$n_{ref}=4$	$n_{ref}=5$	$n_{ref}=6$
$t=0.001$	14.3	9.4	6.6	4.8	4.5	5.0	5.8
$t=0.004$	10.4	6.8	4.9	4.5	4.9	5.2	6.0
$t=0.016$	7.6	5.1	4.6	4.8	5.0	5.2	5.9
$t=0.064$	5.5	4.8	4.8	4.9	5.0	5.1	5.7
$t=0.256$	5.0	4.6	4.5	4.6	4.6	4.7	5.2
$t=1.000$	3.5	3.9	4.2	4.4	4.5	4.6	5.1

Table 2: The effectivity index $\Theta_2^h(t)$ with $c_2^{bou} = 12 \cdot c_2^{int}$

	$n_{ref}=0$	$n_{ref}=1$	$n_{ref}=2$	$n_{ref}=3$	$n_{ref}=4$	$n_{ref}=5$	$n_{ref}=6$
$t=0.001$	10.5	6.4	4.3	3.0	2.4	2.5	2.8
$t=0.004$	7.7	4.6	3.1	2.5	2.5	2.6	2.9
$t=0.016$	5.5	3.4	2.7	2.6	2.6	2.6	3.0
$t=0.064$	3.6	2.9	2.8	2.7	2.7	2.8	3.1
$t=0.256$	2.9	2.4	2.3	2.3	2.3	2.3	2.6
$t=1.000$	2.0	2.0	2.0	2.0	2.0	2.0	2.3

Table 3: The effectivity index $\Theta_2^h(t)$ with $c_2^{int} = c_2^{bou}$

5.2 The performance of the local error indicators

In the previous section we have observed the performance of the (global) error estimators $\mathcal{E}_i(u^h(t))$; in this section we try to asses the (local) error indicators $\eta_{i,E}(u^h(t))$. We remark once more here that, although it is important to have a good approximation of the global error, it is essential (when steering adaptivity) to have the best possible information on the way the error is spread over the domain. In fact, it might be possible to overcome a not too precise estimation of the global error, but it is extremely difficult (even impossible) to perform adaptivity without accurate local error indicators. For example, if an approximation of the global error overestimates the error (most of the global error estimators do so) a feasible remedy is to restrict the number of possible refinements. But steering adaptivity based on information obtained from an inaccurate local error indicators might end in refining regions of the domain where it is not necessary and not refining where it is actually needed.

Our results in this section are based on the solution of the same problem of Section 5.1 when fixing the number of refinement to 5: this corresponds to subdivide in $4 \cdot 2^5$ equal interval the boundary $\partial\Omega$ and in $4 \cdot 4^5$ triangles the domain Ω – similar results were obtained also for coarser triangulations. Note that $n_{ref} = 5$ corresponds to the finer triangulation where we do not see the influence of the reference solution when calculating the "true" errors.

Figure 3 shows, at different time levels, the solution u_1^h, the square of the energy norm of the error element by element (i.e. $\int_E |D_1(\nabla u_1 - \nabla u_1^h)|^2$) and the local error indicator $\eta_{1,E}^2$. For a better layout of the plot, in Figure 3 the boundary $\partial\Omega$ has been cut at point $(-1,-1)$ and opened into a straight line. The four peaks (the first and the last one should be seen as the two halves of the same peak) correspond to the four corners of the square. Clearly, the error is concentrated in the elements where the solution u_1 has steep gradients. The (local) error indicator $\eta_{1,E}$ detects correctly those elements. Note that to appreciate the details we have used different scales for different pictures.

A similar analysis is done for the (local) error indicator $\eta_{2,E}$. Figure 4 shows, at different time levels, the solution u_2^h, the square of the energy norm of the error element by element (i.e. $\int_E |D_2(\nabla u_2 - \nabla u_2^h)|^2$) and the local error indicator $\eta_{2,E}^2$ (defined in (4.2.b)) with the two different choices of the constants c_2^{int} and c_2^{bou}. The different values of c_2^{int} and c_2^{bou} are the same as used in the previous subsection: the case $c_2^{int} = c_2^{bou}$ is plotted in the last column while the situation with $c_2^{bou} = 12 c_2^{int}$ is shown in the third one. Clearly the local indicator corresponding to the choice of different constants c_2^{int}, c_2^{bou} better reproduces the location of the error. We remark here that, according to [16], we have obtained with $c_2^{int} = 0$, $c_2^{bou} = \frac{1}{D_2}$, an error indicator which is essentially equal to the case $c_1^{int} = \frac{1}{12 D_1}$ and $c_2^{bou} = \frac{1}{D_2}$. Figure 5 shows a detail of Figure 4: the error (left) and the indicator $\eta_{2,E}$ with $c_2^{bou} = 12 \cdot c_2^{int}$ (right) at time $t = 0.64$. According to remark (EE1),

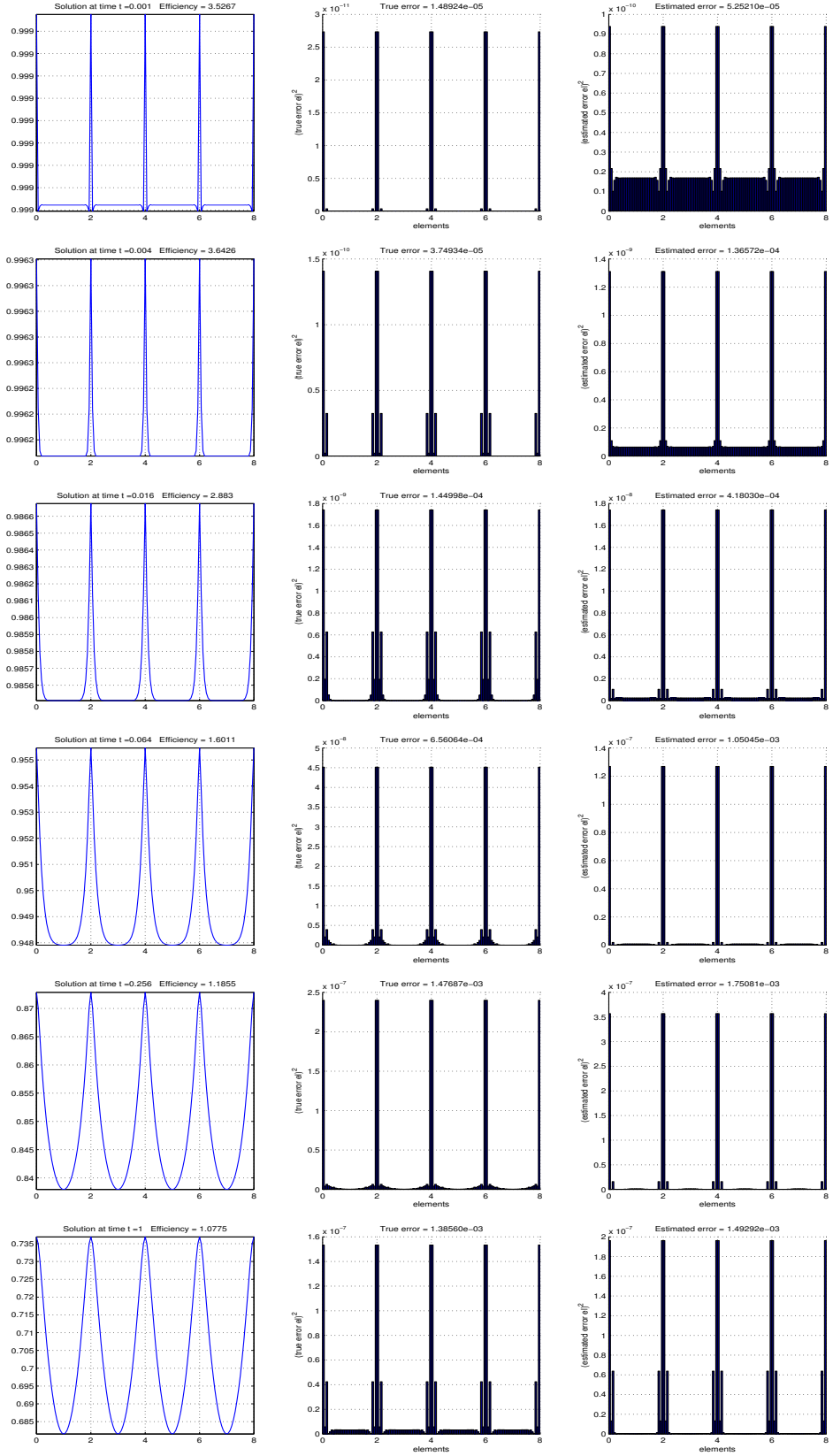

Figure 3: The solution u_1^h (left), the square of error element by element, i.e., $\int_E |D_1(\nabla u_1 - \nabla u_1^h)|^2$ (center), and the error indicator $\eta_{1,E}^2$ (right)

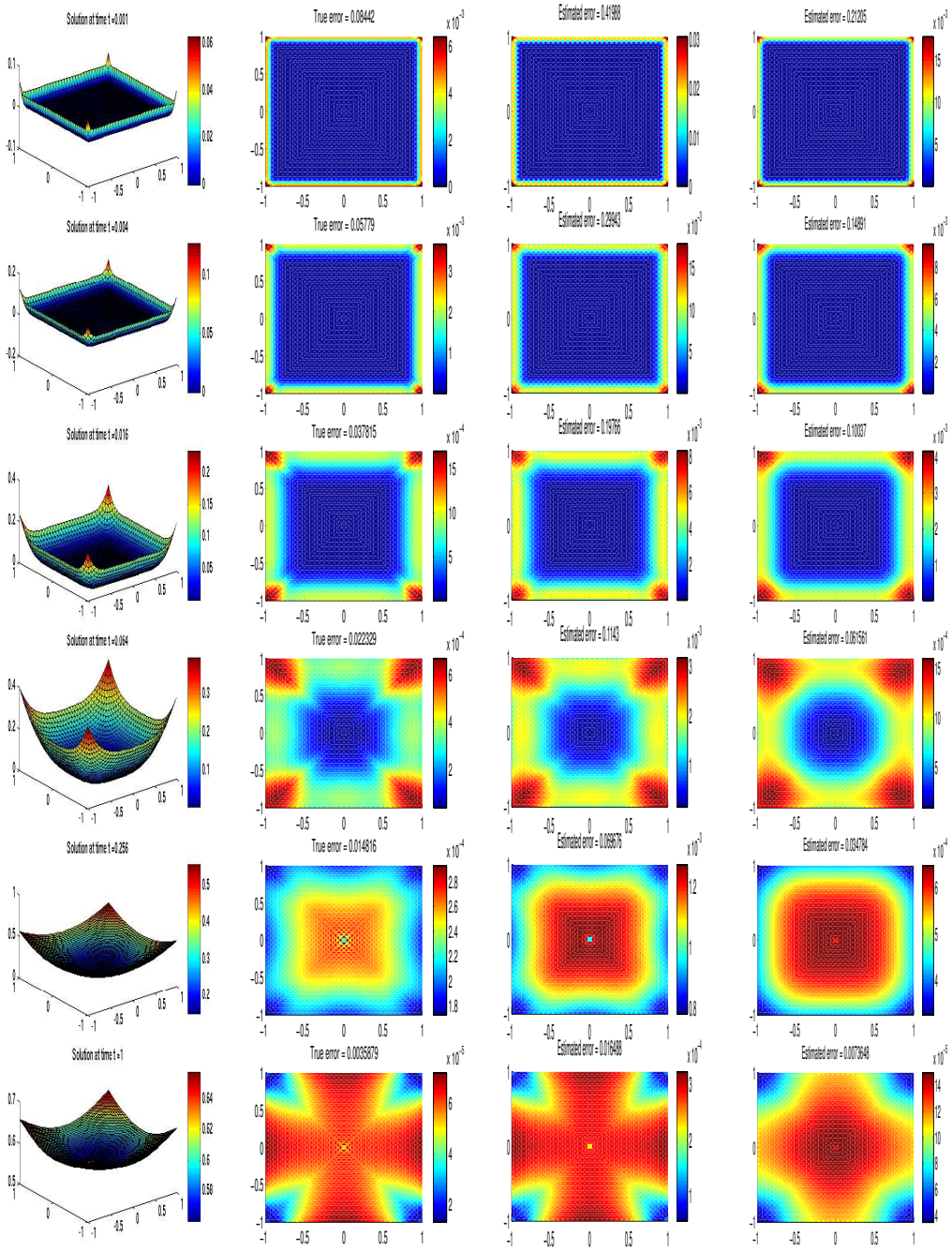

Figure 4: The solution u_2^h (column 1), the square of error element by element, i.e., $\int_E |D_2(\nabla u_2 - \nabla u_2^h)|^2$ (column 2) and the error indicator $\eta_{2,E}^2$ with $c_2^{bou} = 12 \cdot c_2^{int}$ (column 3) and with $c_2^{int} = c_2^{bou}$ (column 4).

the error indicator suffers from the approximation of the boundary conditions: this is particularly evident for the elements attached to the boundary.

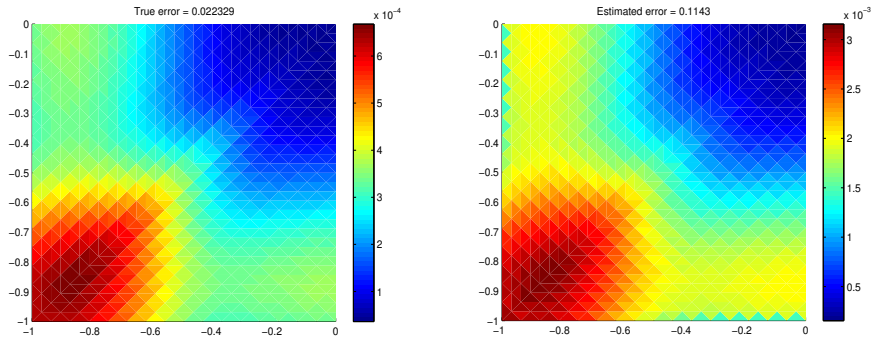

Figure 5: Details of the error (left) and of the error indicator $\eta_{2,E}$ with $c_2^{bou} = 12 \cdot c_2^{int}$ (right) at time $t = 0.064$.

5.3 The performance of the adaptive algorithm

In this section we examine the performance of the error estimation and the adaptive strategy while automatically searching for an optimal triangulation in two slightly different tests.

Test 1

In the first test we apply the adaptive FEMOL of Section 4.2 to the same problem of Section 5.1 and Section 5.2. in order to appreciate the improvement due to the possibility to modify the triangulation *when* and *where* it is necessary

We have fixed here the tolerance constants as follow: $Tol_i^R = 2 \cdot 10^{-1}$, $Tol_i^A = 2\sqrt{2} \cdot 10^{-1}$. This choice will allow us to gives an easy and fair comparison with the results of the previous two sections.

Figure 6 shows, at different time levels, the mesh (and the corresponding solutions u_1^h and u_2^h) generated by the adaptive algorithm. Here we have fixed the parameters $c_1^{int} = \frac{1}{12D_1}$ and $c_2^{bou} = 12c_2^{int} = \frac{1}{D_2}$ (as Sections 5.1 and 5.2). Moreover, we have employed the maximum strategy with $\theta = 0.7$ and regular refinement – see remarks (AA4) and (AA2). Similar results were obtained with different strategies and slightly more graded meshes with longest refinement.

It is interesting to look at the degrees of freedom which are necessary to guarantee, at any time level, the prescribed error tolerance. The adaptive method reaches the prescribed error tolerance with a number of triangles which ranges between 1360 at time $t = 0.004$ (corresponding to 128 degrees of freedom for u_1 and 745 for u_2) and 16 at time $t = 1$ (corresponding to the triangulation $\mathcal{T}_{Base}$ with 8 degrees of freedom for u_1 and 13 for u_2). On the other hand, as we have seen in Section 5.1, to ensure that at any time the estimated error stay below $2 \cdot 10^{-1}$ it was necessary to employ a uniform mesh with $4^7 = 16384$ triangles (corresponding to 256 degrees of freedom for u_1 and 8321 for u_2). Although in assessing the performance of the adaptive FEMOL other parameters have to be taken into account (e.g. computational time) the advantage of the adaptive approach is undeniable: a reduction of the degrees of freedom between 10 and 400 times is very significant.

Test 2

It can be noted that in the first test the refinement of the triangulation is mainly steered by the second species u_2. To better explore the potentials of the adaptive procedure, in the second test we modify the initial condition of the first test problem to

$$u_1^0(x,y) = \begin{cases} 1 & \text{if } x = -1, 1,\ y \in [-\frac{1}{2}, \frac{1}{2}] \\ 0 & \text{otherwise.} \end{cases} \tag{5.2.a}$$

$$u_2^0(x,y) = \begin{cases} \frac{1}{2} & \text{if } x^2 + y^2 \leq \frac{1}{4} \\ 0 & \text{otherwise.} \end{cases} \tag{5.2.b}$$

(5.2.c)

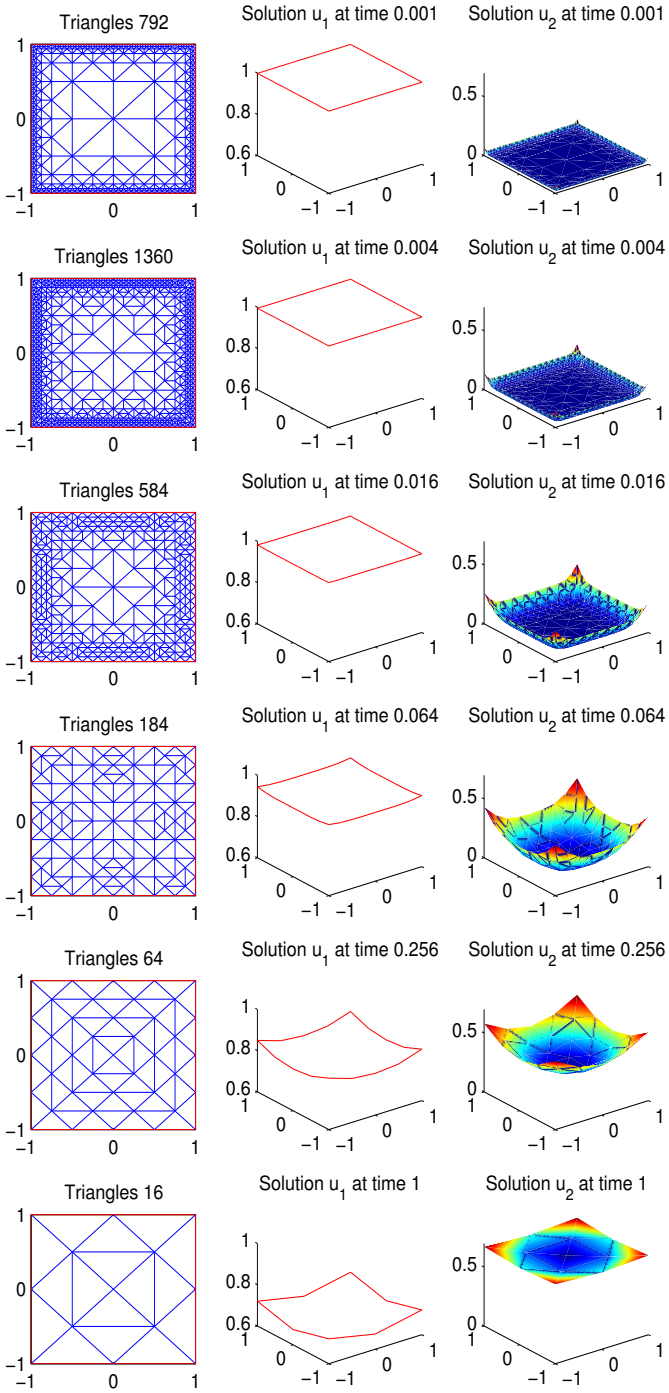

Figure 6: *Test 1*: automatically adapted triangulations (left) and corresponding solutions u_1 (center) and u_2 (right) at different time levels.

With such initial conditions the error estimators and the adaptive procedure will have to deal with steep gradients at the four points $(-1,-\frac{1}{2})$, $(-1,\frac{1}{2})$, $(1,-\frac{1}{2})$, $(1,\frac{1}{2})$ for species u_1 and at the circle of equation $x^2+y^2=\frac{1}{4}$ for species u_2. Once more we have set the tolerances to $Tol_i^R = 2\cdot 10^{-1}$, $Tol_i^A = 2\sqrt{2}\cdot 10^{-1}$, and we have used the maximal error strategy with $\Theta = 0.7$ combined with regular refinement (see remarks (AA3) and (AA4) point (iii)). Similar results were obtained with different strategies and longest refinement. Figure 7 shows, at different time levels, the mesh

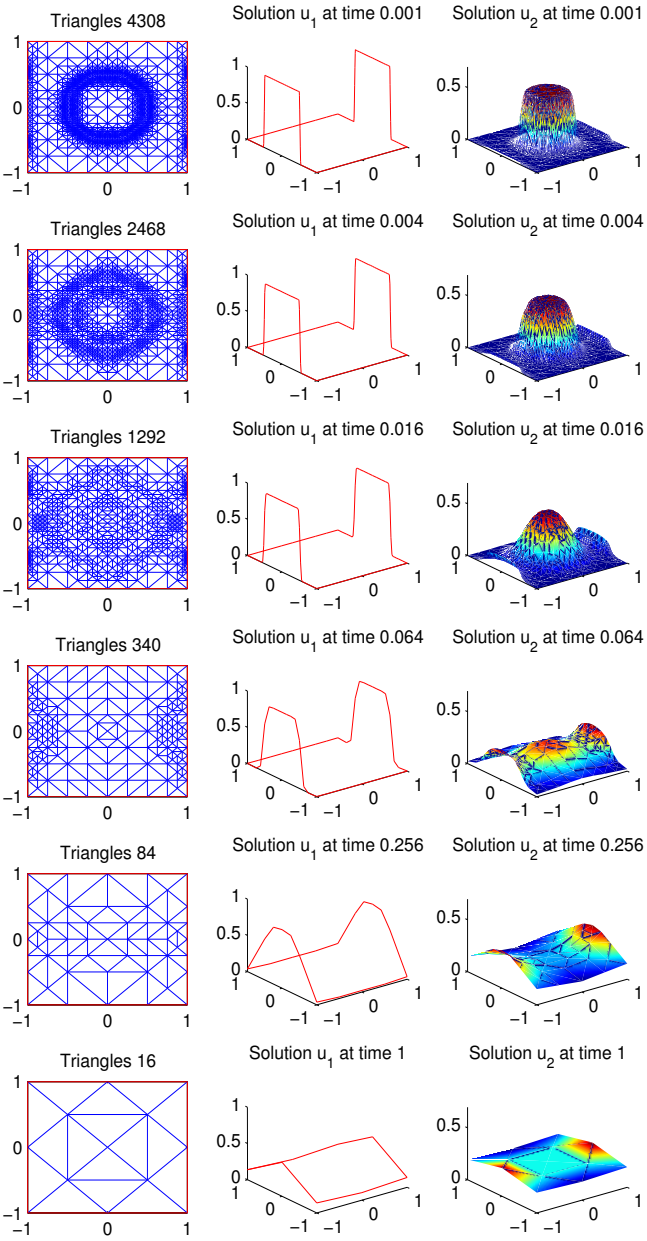

Figure 7: *Test 2*: automatically adapted triangulations (left) and corresponding solutions u_1 (center) and u_2 (right) at different time levels.

(and the corresponding solutions u_1 and u_2) generated by the adaptive algorithm. Once more the adaptive algorithm succeeded in determining *when* and *where* to use a finer mesh.

6. Conclusion

In this note we have investigated the adaptive finite element method of lines (Sections 3 and 4) when applied to a system of reaction-diffusion equations coupling species defined on the whole 2-dimensional domain Ω and species confined to the boundary of the domain $\partial\Omega$ (Section 2). For clarity, the numerical studies were conducted using piecewise linear elements on a model problem with two equations.

The primary interest was the effect of the coupling Ω–$\partial\Omega$ on the performance of the error estimation (Section 4.1) and the successive adaptive process (Section 4.2). We have shown that an adaptive finite element method of lines based on an explicit a-posteriori error estimators (and indicators) can constitute a good compromise between high resolution and limited computational complexity. The experiments presented (Section 5) show that the global estimators are reasonable accurate, the local error indicators are reliable and the adaptive strategy successfully controls the space discretization error.

The application of the method discussed in this paper to systems with more equations is straightforward while the extensions to higher order elements or higher dimensional case require only the calibration (or possibly a new estimate) of the constants weighting the internal and the boundary residuals.

Finally, the simplifications that were introduced at the present stage will be further investigated. We hope to address, in the future, more realistic situations involving a larger number of species in complex domains. Besides, interesting questions like a more careful choice of the Clement's constants, how best to balance the time and space discretization error, the influence of a simple interpolation at nodal points instead of an L_2 projection and the usage of a real coarsening routine, have not been adequately addressed here. We hope to come back to these, and other, challenging issues in forthcoming work.

Acknowledgments

The author would like to thank J.G. Blom and prof. J.G. Verwer for inspiring discussions and carefully reading preliminary versions of the manuscript.

References

1. S. Adjerid, J. E. Flaherty, I. Babuška, A posteriori error estimation for the finite element method-of-lines solution of parabolic problems, Math. Models Methods Appl. Sci. 9 (2) (1999) 261–286.
2. S. Adjerid, J. E. Flaherty, Y. J. Wang, A posteriori error estimation with finite element methods of lines for one-dimensional parabolic systems, Numer. Math. 65 (1) (1993) 1–21.
3. M. Ainsworth, J. T. Oden, A posteriori error estimation in finite element analysis, Pure and Applied Mathematics (New York), Wiley-Interscience [John Wiley & Sons], New York, 2000.
4. M. Ashyraliyev, J. G. Blom, J. G. Verwer, On the numerical solution of diffusion-reaction equations with singular source terms, Tech. Rep. MAS-E0512, Centrum voor Wiskunde en Informatica (CWI), Amsterdam, The Netherlands (July 2005).
5. I. Babuška, R. Durán, R. Rodríguez, Analysis of the efficiency of an a posteriori error estimator for linear triangular finite elements, SIAM J. Numer. Anal. 29 (4) (1992) 947–964.
6. I. Babuška, M. Feistauer, P. Šolín, On one approach to a posteriori error estimates for evolution problems solved by the method of lines, Numer. Math. 89 (2) (2001) 225–256.
7. I. Babuška, M. Vogelius, Feedback and adaptive finite element solution of one-dimensional boundary value problems, Numer. Math. 44 (1) (1984) 75–102.
8. W. Bangerth, R. Rannacher, Adaptive finite element methods for differential equations, Lectures in Mathematics ETH Zürich, Birkhäuser Verlag, Basel, 2003.
9. M. Berzins, P. J. Capon, P. K. Jimack, On spatial adaptivity and interpolation when using the method of lines, in: Proceedings of the International Centre for Mathematical Sciences Conference on Grid Adaptation in Computational PDEs: Theory and Applications (Edinburgh, 1996), vol. 26, 1998.

10. M. Bieterman, I. Babuška, The finite element method for parabolic equations. I. A posteriori error estimation, Numer. Math. 40 (3) (1982) 339–371.
11. M. Bieterman, I. Babuška, The finite element method for parabolic equations. II. A posteriori error estimation and adaptive approach, Numer. Math. 40 (3) (1982) 373–406.
12. M. Bieterman, I. Babuška, An adaptive method of lines with error control for parabolic equations of the reaction-diffusion type, J. Comput. Phys. 63 (1) (1986) 33–66.
13. J. G. Blom, M. A. Peletier, Diffusive gradients in the PTS system, Report MAS-R0020, Centrum voor Wiskunde en Informatica (CWI), Amsterdam, The netherlands (July 2000).
14. A. G. Butkovskiy, Green's functions and transfer functions handbook, Ellis Horwood Ltd., Chichester, 1982, translated from the Russian by L. W. Longdon, Ellis Horwood Series in Mathematics and its Applications.
15. C. Carstensen, S. A. Funken, Constants in Clément-interpolation error and residual based a posteriori error estimates in finite element methods, East-West J. Numer. Math. 8 (3) (2000) 153–175.
16. C. Carstensen, R. Verfürth, Edge residuals dominate a posteriori error estimates for low order finite element methods, SIAM J. Numer. Anal. 36 (5) (1999) 1571–1587 (electronic).
17. P. G. Ciarlet, The finite element method for elliptic problems, North-Holland Publishing Co., Amsterdam, 1978, studies in Mathematics and its Applications, Vol. 4.
18. P. Clément, Approximation by finite element functions using local regularization, RAIRO Analyse Numérique 9 (R-2) (1975) 77–84.
19. M. Dauge, Elliptic boundary value problems on corner domains, vol. 1341 of Lecture Notes in Mathematics, Springer-Verlag, Berlin, 1988, smoothness and asymptotics of solutions.
20. W. Dörfler, A robust adaptive strategy for the nonlinear Poisson equation, Computing 55 (4) (1995) 289–304.
21. K. Eriksson, D. Estep, P. Hansbo, C. Johnson, Introduction to adaptive methods for differential equations, in: Acta numerica, 1995, Acta Numer., Cambridge Univ. Press, Cambridge, 1995, pp. 105–158.
22. K. Eriksson, C. Johnson, Adaptive finite element methods for parabolic problems. I. A linear model problem, SIAM J. Numer. Anal. 28 (1) (1991) 43–77.
23. K. Eriksson, C. Johnson, Adaptive finite element methods for parabolic problems. IV. Nonlinear problems, SIAM J. Numer. Anal. 32 (6) (1995) 1729–1749.
24. D. J. Estep, M. G. Larson, R. D. Williams, Estimating the error of numerical solutions of systems of reaction-diffusion equations, Mem. Amer. Math. Soc. 146 (696) (2000) viii+109.
25. C. Francke, P. W. Postma, H. V. Westerhoff, J. G. Blom, M. A. Peletier, Why the Phosphotransferase System of *Escherichia Coli* Escapes Diffusion Limitation, Biophys. J. 85 (1) (2003) 612–622, revised version of CWI Report MAS-R0218.
26. J. Lawson, M. Berzins, P. M. Dew, Balancing space and time errors in the method of lines for parabolic equations, SIAM J. Sci. Statist. Comput. 12 (3) (1991) 573–594.
27. R. Sandboge, Adaptive finite element methods for systems of reaction-diffusion equations, Comput. Methods Appl. Mech. Engrg. 166 (3-4) (1998) 309–328.
28. K. Segeth, A posteriori error estimates for parabolic differential systems solved by the finite element method of lines, Appl. Math. 39 (6) (1994) 415–443.
29. K. Segeth, A posteriori error estimation with the finite element method of lines for a nonlinear parabolic equation in one space dimension, Numer. Math. 83 (3) (1999) 455–475.
30. A.-K. Tornberg, B. Engquist, Numerical approximations of singular source terms in differential equations, J. Comput. Phys. 200 (2) (2004) 462–488.
31. R. Verfürth, A review of a posteriori error estimation and adaptive mesh-refinement techniques, Wiley-Teubner Series Advances in Numerical Mathematics, John Wiley & Sons Ltd and B. G. Teubner, Chichester and Stuttgart, 1996.